Journal of Materials Chemistry C

Accepted Manuscript

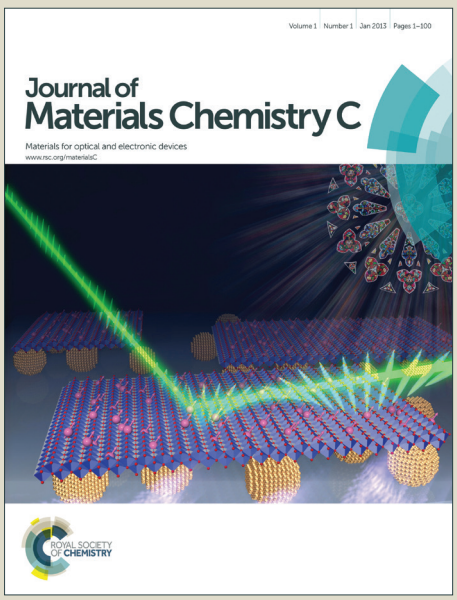

ROYAL SOCIETY OF CHEMISTRY

www.rsc.org/materialsC

Journal Name

RSCPublishing

ARTICLE

The 2-Phenylbenzimidazole-5-sulfonate/layered double hydroxides co-intercalation composites and its luminescence response for nucleotides

Cite this: DOI: 10.1039/x0xx00000x

Received 00th January 2012,
Accepted 00th January 2012

DOI: 10.1039/x0xx00000x

www.rsc.org/

Shufang Zheng, Jun Lu *,Wu Li,Yumei Qin, Dongpeng Yan, David G Evans, and Xue Duan

The fluorescence sensing for nucleotides is an important topic for biosensor and fluorescence materials. In this paper, a cheap UV light absorber, 2-Phenylbenzimidazole-5-sulfonate(PBS) was immobiled into the interlayers of Zn_2Al layered double hydroxides(LDHs) by co-intercalating with 1-decane sulfonate (DES) anions. The fluorescence dependance on the molar concentration (x%) of PBS was investigated and the PBS(15%)-DES/LDH composite exhibited the optimal violet luminescence at 402 nm, compared with that of PBS solution with luminescence at 342 nm. The PBS(15%)-DES/LDH composite thin films were fabricated by solvent evaporation method on quartz substrate. Moreover, the composite thin film exhibited the remarkable PBS luminescence transformation (violet to UV light) for nucleotides triphosphate (ATP, GTP, CTP and UTP), compared with their diphosphate and monophosphate counterparts (ADP, AMP and etc.), which is expected to be prospective for sensing the nucleotide molecules at the simulated physiological conditions. The origin of the luminescence enhancement was investigated and attributed to the extensive hydrogen bonding interaction between the intercalated PBS and nucleotides.

Introduction

In recent years, the development of molecular-recognition and sensing systems for biologically important anions has received considerable attention. [1-8] As one of the nucleotides, adenosine triphosphate (ATP) molecules play an indispensable role in the biochemical process, which was not only a universal energy source in the biochemical reactions, but also an extracellular signaling mediator in many biological processes.[9] Guanosine trisphosphate (GTP) was involved in RNA synthesis, citric acid cycle, and acts as an energy source for protein synthesis.[10] Moreover, other nucleoside poly-phosphates, such as adenosine monophosphate (AMP), adenosine diphosphate (ADP) and guanosine monophosphate (GMP), also play pivotal roles in various physiological events. For example, AMP and ADP were vital in bioenergetics, metabolism, and transfer of genetic information, and GMP acts as an intermediate in the synthesis of nucleic acids and has a crucial role to perform in several metabolic processes. [11] CDP and CTP is also a kind of energetic compounds, which take part in the biological phospholipid metabolism in the body. On the other hand, uridine triphosphate (UTP) and uridine diphosphate (UDP), the key building blocks for RNA synthesis, were widespread in living cells and featured in various biological events. [12] The recognition and sensing of nucleotides like ATP has been an active research focus for academic research and applications.

Up to now, many methods have been developed for the detection of nucleotides, among which the fluorescence sensing progressed rapidly due to the advantage of high sensitivity, lossless determination, fast, low cost, easy to operate. For example, Yoon *et al*. [7] investigated a pincer-like benzene-bridged sensor with a pyrene excimer as a signal source and imidazolium as a phosphate anion receptor for ATP sensing. Ones such as azacrown, amide and urea derivatives were found to detect nucleotides based on hydrogen bond interactions. In 2006, Bazzicalupi and Bencini *et al*. reported a new phenanthroline-containing macrocycle which could selectively recognize and sense ATP among triphosphate nucleotides at pH 6. [13] One also use the metal complexes like zinc (Zn^{2+}), ytterbium (Yb^{3+}), ruthenium (Ru^{2+}), europium (Eu^{3+}), terbium (Tb^{3+}), yttrium (Y^{3+}), manganese(Mn^{2+}) or cobalt (Co^{2+}) as the binding motif to detect nucleotides,.[8] Even more, polymers or mesoporous materials can be used as nucleotides sensors. Shinkai's group[14] reported a water-

soluble cationic polythiophene derivative which displayed colorimetric and fluorescent responses to ATP through electrostatic and hydrophobic cooperative interactions. All of the methods were rather complex, expensive and/or one-off for sensing. The repeatable and high performance devices detection is needed for practical nucleotides probe. Furthermore, it is still a challenge for these sensor materials to discriminate a certain nucleotide triphosphate among others.

Recently, considerable interest has been focused on the fabrication of 2D ordered organic-inorganic thin film materials, for they may show novel functionalities (such as enhanced photo-, thermal-, and mechanical-stability) compared with their individual components alone.[15,16] In this sense, layered double hydroxides (LDHs), whose structure can be generally expressed as the general formula $[M^{II}_{1-x}M^{III}_{x}(OH)_2]^{z+}A^{n-}_{z/n}\cdot yH_2O$($M^{II}$ and M^{III} are divalent and trivalent metals respectively, A^{n-} is the guest anion), were one type of important layered matrixes with the various interlayer anions, and the adjustable interlayer spacing.[17-21] Various negative-charged species including DNA and nucleotides have been intercalated into the LDHs [22,23].

The 2-Phenylbenzimidazole-5-sulfonic acid (PBS) is an kind of ultraviolet light absorber due to its outstanding UV light absorption ability[24], and it has extensive applications in cosmetics and rubber industry. Its π-conjungated electon system involving benzene ring and imidazole group made it well blue fluorophore, and the PBS powder and solution luminesces at 450 nm and 340 nm, respectively, which no attention was paid to being a sensor for biomolecules.

Herein, PBS anions were introduced into the interlayers of Zn_2Al-LDHs by co-intercalating with decane-1-sulfonate (DES) anions to form the PBS(x%)-DES/LDHs composite system . The strongest fluorescence was found to be PBS(15%)-DES/LDHs at 402 nm, with a blue shift of about 50 nm compared with PBS powder. The PBS(15%)-DES/LDHs composite thin film on quartz substrates was fabricated by the drop-casting method, which show the 402 nm luminescence on-off switch response for the ATP physiological solution with concentration range from 10^{-3} to 10^{-7} M. Furthermore, accompanied with the quenching of 402 nm luminescence, the strong 342 nm UV luminsecence appears, which is more obvious for sensing ATP than ADP/AMP, and is held for other nucleotides (CXP, GXP, and UXP). Therefore, this composite thin film can fluorescent special detect the nucleoside triphospates. This a simple, repeatable and fast detecting approach for sensing nucleotides.

Experimental Section

Reagents and Materials

2-Phenylbenzimidazole-5-sulfonic acid ($C_{13}H_9N_2O_3SNa$, PBS), Sodium decane-1-sulfonate ($C_{10}H_{21}O_3SNa$, DES), 5'-adenosinetriphosphate disodium salt ($C_{10}H_{14}N_5O_{13}P_3Na_2$, ATP), 5'-adenyldiphosphate disodium salt ($C_{10}H_{13}N_5O_{10}P_2Na_2$, ADP), adenosine-5'-monophosphate disodium salt ($C_{10}H_{12}N_5O_7PNa_2$, AMP), uridine-5'-triphosphate trisodium salt dihydrate ($C_9H_{12}N_2O_{15}P_3Na_3\cdot 2H_2O$, UTP), uridine-5'-diphosphate sodium salt ($C_9H_{14}N_2O_{12}P_2Na_2\cdot 2H_2O$, UDP), Uuridine-5'-monophosphate disodium salt ($C_9H_{11}N_2O_9PNa_2\cdot xH_2O$, UMP), cytidine 5'-triphosphate disodium salt ($C_9H_{14}N_3O_{14}P_3Na_2$, CTP), cytidine 5'-diphosphate trisodium salt hydrate ($C_9H_{12}N_3O_{11}P_2Na_3\cdot xH_2O$, CDP), cytidine 5'-monophosphate disodium salt ($C_9H_{14}N_3O_8PNa_2$, CMP), Guanosine 5-triphosphate disodium salt ($C_{10}H_{14}N_5O_{14}P_3Na_2$, GTP), guanosine 5′-diphosphate sodium salt($C_{10}H_{14}N_5O_{11}P_2Na$, GDP), guanosine 5'-monophosphate disodium salt ($C_{10}H_{12}N_5O_8PNa_2$, GMP) and (2-[4-(2-hydroxyethyl)-1-pipera-zinyl] ethane sulfonic acid) ($C_8H_{18}N_2O_4S$, HEPES) were purchased from J&K Chemical Co. Ltd. Analytical grade $Zn(NO_3)_2\cdot 6H_2O$, $Al(NO_3)_3\cdot 9H_2O$, and NaOH were purchased from Beijing Chemical Co. Ltd. All other chemicals were analytical grade and used as received without further purification. Deionized water was used throughout the experimental process.

Preparation of PBS(*x*%)-DES/LDH composites

The PBS(*x*%)-DES/LDH powder was synthesized by the co-precipitation method reported previously.[25] $Zn(NO_3)_3\cdot 6H_2O$(0.01mol) and $Al(NO_3)_2\cdot 9H_2O$(0.005mol) were dissolved in ethanol-deionized/deCO_2 water (v/v 1:1) mixture as solution A, PBS (a mol), DES (b mol in which a + b = 0.005 mol, *x* % = a /(a + b), *x* % = 10, 15, 20, 25, 30, 50, 75, and 100 %, respectively) and NaOH (0.03 mol) were dissolved in ethanol-deionized/deCO_2 water (v/v, 1:1) mixture as solution B. Then the solution B was added into solution A with the dropping rate of 10 d/min by using the seal funnel under the protection of N_2 atmosphere. The product then was aged in 100 ml PTFE-lined autoclave at 100 °C for 20 h. Then the white powder product was obtained by centrifugation, washing and drying.

Fabrication of PBS(15%)-DES/LDHs thin films and its detection of nucleotides

The PBS(15%)-DES/LDH composite thin film was prepared by the drop-casting method.[26] The suspension of the PBS(15%)/DES-LDH composite in ethanol (1mg/mL) was thoroughly dispersed by an ultrasonicator under a N_2 atmosphere for 15 min. After filtration using a membrane filter (0.2 μm, Millipore), 5 mL of the PBS(15%)/DES-LDH ethanol suspension was dropped onto a quartz substrate and dried in vacuum at ambient temperature to the thin films. Then detecting the change of the fluorescence before and after dipping it into the

nucleotides physiological solutions (10^{-3}–10^{-7}M, pH = 7.4 in 10mM HEPES solution) for 4 min.

Characterization

The analysis of metal contents was performed by ICP atomic emission spectroscopy (AES) on a Shimadzu ICPS-7500 instrument using solutions prepared by dissolving the samples in dilute nitric acid. Carbon, hydrogen and nitrogen analyses were carried out using a Perkin Elmer Elementarvario elemental analysis instrument. X-ray diffraction patterns (XRD) of the PBS-DES/LDH composites were recorded by using a Shimadzu XRD-600 diffractometer under the conditions: 40 kV, 50 mA, Cu Kα radiation (λ = 0.154056 nm) with step-scanned in step of 0.04°/2θ in the range from 3 to 70°, and a count time of 10 s/step. Thermo-gravimetry and differential thermal analysis (TG-DTA) measurement was performed on the PBS/LDHs with APCT-1A thermal analysis system under ambient atmosphere employing a heating rate of 10 °C/min. The morphology of thin films was investigated by using a scanning electron microscope (SEM Hitachi S-3500) and the accelerating voltage applied was 20 kV. The surface roughness and thickness data were obtained by using the atomic force microscopy (AFM) software (Digital Instruments, Version 6.12). The Fourier transform infrared (FT-IR) spectra were recorded by using a Nicolet 605 XB FT-IR spectrometer in the range 4000–400 cm^{-1} with 4cm^{-1} resolution in air. The standard KBr disk method (1 mg of sample in 100 mg of KBr) was used. The UV-vis absorption spectra were collected in the range from 220 to 800 nm on a Shimadzu UV-3600 spectrophotometer, with the slit width of 5.0 nm. The fluorescence spectra were collected on a Hitachi F-7000 fluorospectrophotometer with the excitation wavelength of 300 nm and the emission spectra range in 320 nm to 580 nm, and both the excitation and emission slit are set to 5 nm. The fluorescence decay cure was mearsured on Edinburgh Instruements'FLS 980 fluorimeter with the pulse laser excitation at 300 nm at room temperature. The fluorescnece lifetime, the percentage contribution of each component were calculated by exponentially fitting the fluorescence decay curve with the F980 Edinburgh instruments software.

Results and Discussions

Synthesis of PBS(*x*%)-DES/LDH

The chemical compositions of the resulting products are listed in Table 1, which is inferred from the ICP-AES and elemental analysis. It can be seen that the ratio of divalent to trivalent metal conforms well to the nominal ratio: 1.73–1.91 for Zn_2Al- LDH, and in the range of Zn/Al = 1.0 – 5.0 at pH = 7,[27] indicating that both divalent and trivalent metal quantitatively precipitated during the co-precipitation process. And the observed PBS content (*x*) is less than the initial nominal content before 30.46 %, while more than after that. However, the excess amount trends in final *x* upon the increase of the initial PBS concentration holds throughout the whole concentration range as expected. This abnormal varying trend maybe related with the strong π-π aggregation effect of PBS in higher concentration.

The X-ray powder diffraction patterns of the as-prepared products were shown in Fig. 1, the diffraction peaks were indexed as hexahedral crystal system (space group $R\bar{3}m$), a typical 3*R*-type LDH structure. Curve *a* is the XRD pattern of Zn_2Al-NO_3-LDH and Curve b-i represent PBS (*x*%)-DES/LDHs XRD patterns (*x* = 10 - 100), respectively. As is shown, the 003 diffraction peak of intercalation compounds move to the low angle region compared to the Zn_2Al-NO_3-LDHs. The sharp peak of 003, 006, and 009 present a good multiple relationship and indicates that the crystalline layered structure was held in the whole co-intercalation range. Therefore, it can be concluded that the PBS anion was intercalated successfully and the layered structure of LDHs hold. The layer spacing of PBS(*x*%)-DES/LDHs increased from 2.18 nm (PBS 10%) to 2.22 nm (PBS 25%), then gradually reduced to the minimum 2.04 nm (PBS 100 %) with the increase of PBS initial molar percentage (*x* %). This can be attributed to the different interlayered molecules arrangement of PBS and DES with various concentration. For the extreme component, the PBS only intercalation sample, the XRD of which (100% sample i in Figure 1) showed the good

Table 1 The elemental composition of PBS(*x*%)-DES/LDH

Nominal (*x* %)	Chemical Composition	Zn/Al Ratio	Determined (*x* %)
10	$Zn_{0.656}Al_{0.344}(OH)_2(C_{13}H_9N_2SO_3)_{0.028}(C_{10}H_{21}SO_3)_{0.316}\cdot 1.035H_2O$	1.91	8.14
15	$Zn_{0.654}Al_{0.346}(OH)_2(C_{13}H_9N_2SO_3)_{0.036}(C_{10}H_{21}SO_3)_{0.310}\cdot 1.518H_2O$	1.89	10.40
20	$Zn_{0.650}Al_{0.350}(OH)_2(C_{13}H_9N_2SO_3)_{0.060}(C_{10}H_{21}SO_3)_{0.290}\cdot 1.690H_2O$	1.86	17.14
25	$Zn_{0.654}Al_{0.346}(OH)_2(C_{13}H_9N_2SO_3)_{0.071}(C_{10}H_{21}SO_3)_{0.275}\cdot 1.800H_2O$	1.89	20.52
30	$Zn_{0.652}Al_{0.348}(OH)_2(C_{13}H_9N_2SO_3)_{0.106}(C_{10}H_{21}SO_3)_{0.242}\cdot 2.410H_2O$	1.87	30.46
50	$Zn_{0.645}Al_{0.355}(OH)_2(C_{13}H_9N_2SO_3)_{0.230}(C_{10}H_{21}SO_3)_{0.125}\cdot 3.210H_2O$	1.82	64.90
75	$Zn_{0.634}Al_{0.366}(OH)_2(C_{13}H_9N_2SO_3)_{0.317}(C_{10}H_{21}SO_3)_{0.049}\cdot 2.170H_2O$	1.73	86.71
100	$Zn_{0.650}Al_{0.350}(OH)_2(C_{13}H_9N_2SO_3)_{0.350}\cdot 1.610H_2O$	1.86	100

crystallinity with the apperance of multiple diffraction 00*l*, which implied that the crystallites is well ordered in the stacking *c* direction and the intercalated PBS anions was orientated orderly within the interlayer space due to the strong π-π aggregation effect of PBS.

Fig. 2 displays the FT-IR spectra of the products, in curve a, the 1387 cm^{-1} peak is the stretching vibration of NO_3^- in the ZnAl-NO_3-LDHs and the O-M-O vibration peak appeared at 431cm^{-1}.[24] FT-IR spectrum of PBS powder (curve b) appeared characteristic absorption peak of -SO_3^{-1} at 1200 cm^{-1}. The characteristic absorption peak of -SO_3^{-1} moved to 1184 cm^{-1} (curve c) and 1190 cm^{-1} (curve d) after intercalating into the Zn_2Al-LDHs layers, and the characteristics peak of NO_3^- disappeared, especially in the curve d, 2854 cm^{-1}, 2920 cm^{-1} is the absorption peak for methylene symmetric and anti-symmetric stretching vibration of C-H, corresponding to the co-intercalated surfactant DES. This indicates that the PBS and DES anion has co-intercalated into LDHs layers successfully, and there is strong interaction between the host LDHs layers and the guest molecules.

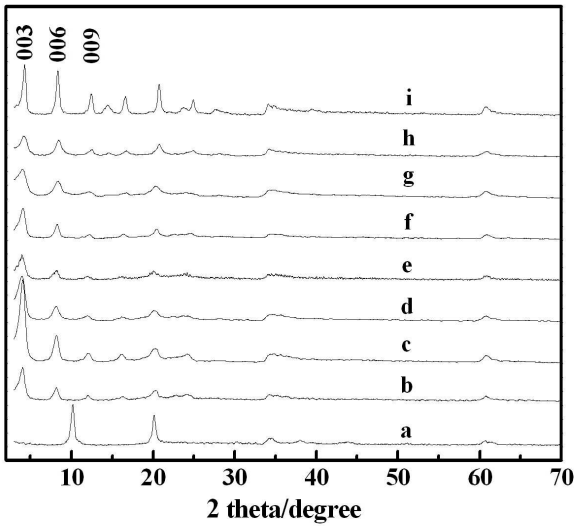

Fig. 1 XRD patterns, a-ZnAl-NO_3-LDH; b-i PBS(*x*%)-DES/LDH (*x* = 10-100%)

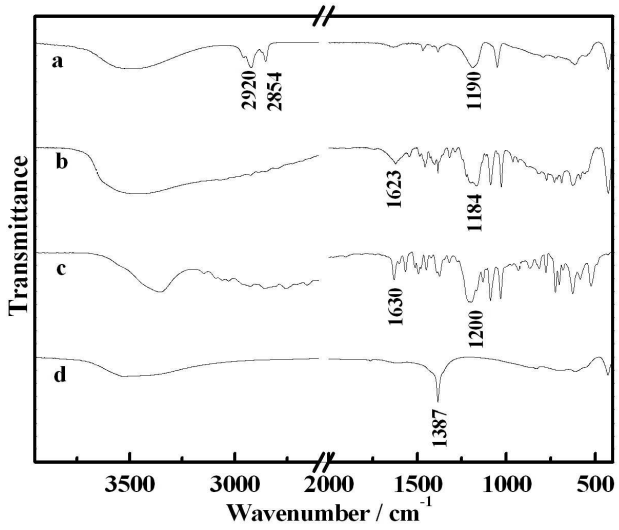

Fig. 2 FT-IR spectra, a- PBS(15%)-DES/LDH ; b- PBS-LDH; c-PBS; d- Zn_2Al-NO_3-LDH

Morphology analysis of PBS(15%)-DES/LDH thin film

The PBS(15%)-DES/LDH thin film was fabricated by the drop-casting method by solvent evaporation, and the resulting scanning electron microscope (SEM) and atomic force microscope (AFM) topographical images are displayed in Fig. 3. The SEM image exhibits a smooth and continuous surface and the PBS(15%)-DES/LDH lamellar crystallites are stacked with the *ab* plane parallel to the substrate in the side view with an average film thickness of *ca*. 2 μm. The average root-mean-square (rms) roughness of the film is about 28 nm, as inferred from the AFM image (scan = 2 μ m × 2 μ m) in Figure 3c, which indicates that the surface of the film is very smooth. The morphology images confirmed that the film is fabricated with an excellent c orientation of PBS-DES/LDH(15%) platelets, consistent with the XRD result (Fig. S1 in ESI).

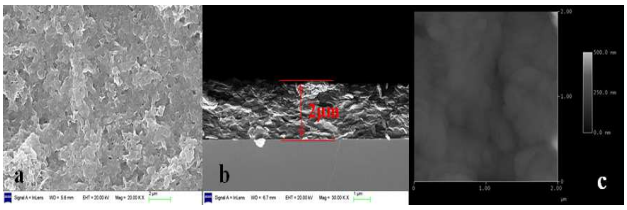

Fig. 3 a) Top and b) side-view SEM images and tapping-mode AFM image (c) of the PBS(15%)-DES/LDH thin film

Fluorescence spectroscopy of PBS(15%)-DES/LDH thin film

The fluorescence emission spectra of PBS-DES/LDH samples with different molar ratios of PBS to DES are

shown in Fig. 4A. The fluorescence intensity increases at first to a maximum (x = 15%), and then decreases with the increase of the PBS content. The optimal luminous intensity presents in the sample with x = 15%, and the emission peak appears at 402 nm with the full width at half maximum (FWHM) of *ca*.50 nm, which corresponds to the S_1–S_0 transition (the transition dipole moment along the long axis direction of PBS).[28] The maximum emission wavelength shifts to 433 nm and its intensity falls quickly when the PBS content increases to 100 %. This peak is different from that of PBS solution with emission maximum peaked at 342 nm. Furthermore, in the sample of x = 10% and 15%, the two shoulder (346 nm, and 364 nm) at high energy can be resolved, which was absent for higher PBS contents. This is contrast with the PBS solution, which show the 342 nm UV fluorescence band(Fig S2 in ESI). This phenomenon can be attributed to the following reasons: the DES/PBS co-intercalated into the interlayer of LDHs formed a hydrophobic environments for PBS, which affect the S_1 excitation state and induced the red-shift of the S_1–S_0 transition. With low PBS concentration, the PBS anions exhibit single molecular luminescence, accounting for the increase in the luminous intensity firstly; the formation of molecular aggregation occurs with further increase in PBS content, resulting in the weak fluorescence intensity and the red shift of emission spectra. The solid state UV-vis absorption spectra of the PBS(x%)-DES/LDH samples are shown in Fig. 4B. The maximum of absorption bands located around 280 nm increases upon the concentration of PBS. Furthermore, an absorption shoulder band at 380 nm appears when the content of PBS increases to 25 %, and the spectra become broad. This can be assigned to the appearance of J-type aggregation of PBS in the galleries of LDH, which is consistent with the red-shift phenomenon in

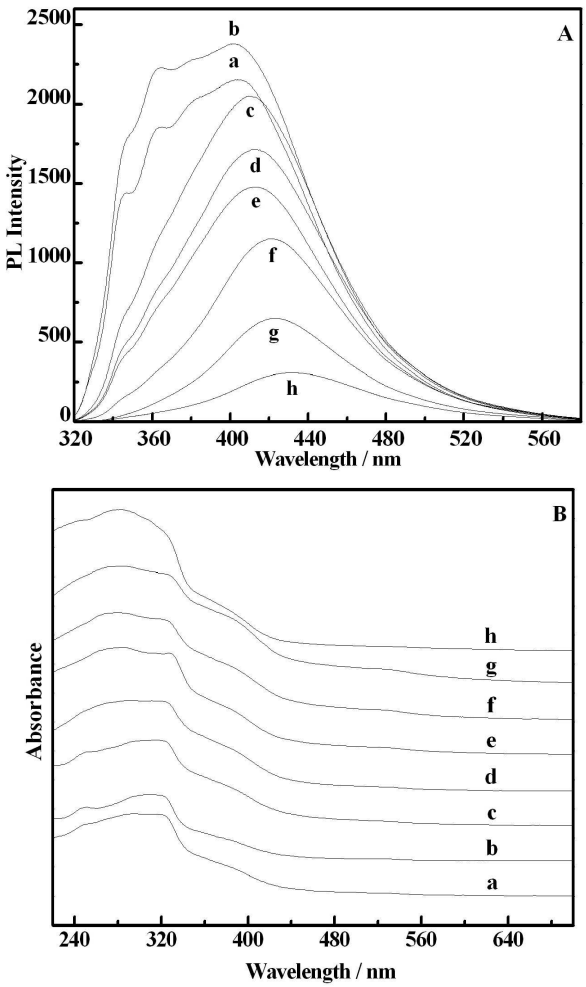

Fig. 4 A. The photoemission spectra of the PBS(x%)-DES/LDH samples with the 300 nm excitation. **B**. The UV-vis absorption spectra of the PBS(x %)-DES/LDH samples with the increase of PBS content (a) 10%, (b) 15%, (c) 20%, (d) 25%, (e) 30%, (f) 50%, (g) 75%, (h) 100%

the fluorescence emission spectra discussed above. Compared with the pristine PBS intercalated LDH system, the PBS aggregation cannot form in the samples with low PBS content, by which the improvement of luminous efficiency can be achieved. It was reported that surfactants or organic solvents can alter the aggregation of photoactivespecies, and the presence of the long-chain surfactant led to a high emission intensity in the system of benzene and imidazole compounds intercalated cation clay.[29] In our opinion, the intercalated long-chain surfactant molecules achieved a homogeneously hydrophobic interlayer environment, which can isolate PBS anions and thus prevent the fluorescence self-quenching.

The luminescence response of PBS(15%)-DES/LDH thin film for nucleotides

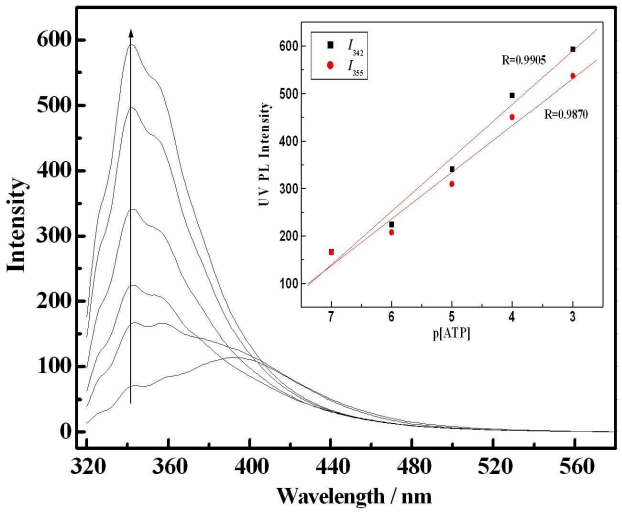

Fig. 5 Variation in the photoemission spectra of PBS(15%)-DES/LDH thin film with increasing concentrations of ATP as indicated in physiological condition (pH = 7.4). Inset: the plot of the UV luminescence intensity at 342 nm and 354 nm to the ATP concentration (p[ATP]= –log[ATP]), which indicates a good linear relationship (the red lines, R=0.9905, 0.9870).

As shown in Fig. 5, the fluorescence emission maximum of PBS(15%)-DES/LDH thin film appears at around 402 nm in dry air. The blank experiment was carried out, and indicated that the PL emission spectra of the film did not show any obvious change in the water. When immersing into the ATP solution, upon increasing the ATP concentration, the fluorescence emission maximum is gradually blue shifted to 342 nm with a dramatic fluorescent transformation from violet luminescence to dark by visual observation (Fig. S3 in ESI) and this transformation was completed within 4 min. The UV luminescence bands peaked at 342 nm and its intensity was linearly responsed to the negative logarithm of ATP concentration within 10^{-7} to 10^{-3} M. This two UV luminescence peak are characteristic of PBS solution. These results indicated that the PBS(15%)-DES/LDH thin film could be used as a novel fluorescence sensor for ATP.

In addition, the fluorescence changes of film with ATP was supported by the fluorescence lifetimes measurements, which is shown in Table S1 in ESI. The fluorescence lifetimes of the thin film are 0.711 ns and 3.403 ns at 342 nm and 402 nm respectively with 300 nm excitation. When the film was immersed in the ATP solutions (10^{-4} M), the fluorescence lifetimes at 342 nm was up to 1.452 ns while the fluorescence lifetimes at 400 nm falled to 1.700 ns.

Likewise, the PBS(15%)-DES/LDH thin film can show the fluorescence response to other adenosine nucleotides: ADP and AMP. And the similar phenomena also appeared for the case of ADP and AMP (Fig. 6). The violet fluorescence was quenched by the AXP (10^{-4}M) obviously. Furthermore, It is subtile that the fluorescence response for the three nucleotides is fairly different, ATP quenched the violet fluorescence more than ADP and AMP, and the ADP quenched the violet fluorescence more than AMP. Quantitatively, we can distinguish them by detecting the fluorescence intensity ratio of I_{342}/I_{402} for PBS(15%)-DES/LDH thin film. And the order is 4.88(ATP) > 2.41(ADP) > 1.16(AMP). The photographs of the thin film exposed to dry air or in the AXP(10^{-4} M) solution exhibited this trend visually(Fig. S3 ESI). Distinctly, the PBS(15%)-DES/LDH thin film can detect the presence of nucleotides (ATP, *vs.* ADP, AMP), when the nucleotides are coexisted in the solution (Fig. S4 ESI) and this ratio was 3.89, which implied that the ATP anion contributed most to the fluorescence response.

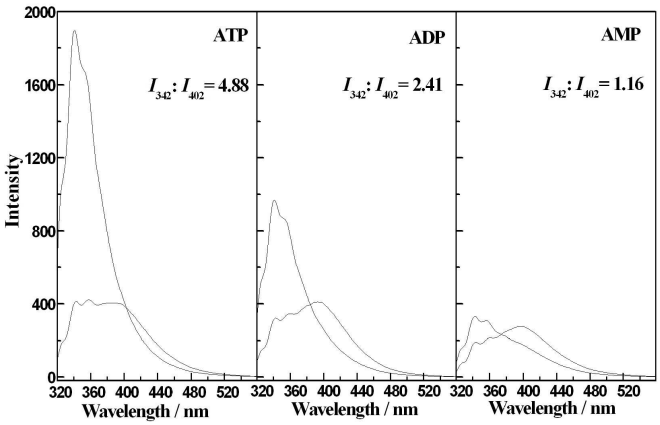

Fig. 6 The fluorescence response of PBS(15%)-DES/LDH thin film to the AXP solution (10^{-4}M) under physiological conditions (10 mM HEPES, pH = 7.4).

Practically, the sensor should work repeatedly without lossing sensitivity. As for the PBS(15%)-DES/LDH thin film, the recycle examination was carried out by immersing the thin film into the ATP solution (10^{-4} M) for 4 min, measuring the fluorescence spectra and then air-drying, measuring again. This immersing/air-drying cycle process was repeated as many times as possible. It was found that its fluorescence response to nucleotides was held for 5 recycles at least (Fig. 7 and Fig. S5 in ESI). Obviously, this ability of iterative sensoring for nucleotides was attributed to the immobilization for PBS anions within the interlayers of LDHs.

Moreover, this response was investigated into other nucleotides in physiological condition, including UXP, GX P and CXP. Our results indicates that the identical rule for ATP/ADP/AMP adapted to these nucleotides homologues (Fig.S6, Table S2 in ESI). That is, the PBS-DES/LDH(15%) thin film exhibited the greater I_{340}/I_{402} ratio for nucleotides trisphosphate, than their diphospahte and monophosphate counterparts which is generally adapted to all the four nucleotides.

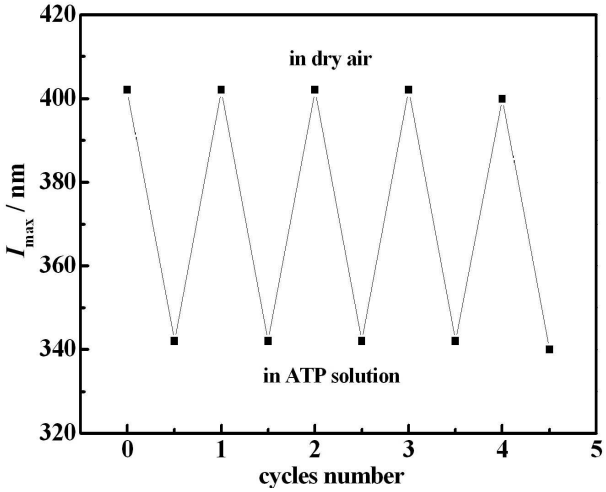

Fig. 7 The fluorescence response repeatability of the PBS(15%)-DES/LDH thin film to the ATP solution

The mechanism of fluosrescence response of PBS(15%)-DES /LDH thin film for nucleotides

This effect made us to speculate the interaction between the unique intercalated PBS anions and nucleotides by taking the intercalated LDHs structures into consideration. The 402 to 342 nm fluorescence transformation was absent for PBS/AXP mixture solution, in which the PBS^- and nucleotides anions cannot approach to each other due to the electrostatic repulsion. Therefore, the nucleotides has little influence on the fluorescence of PBS (Fig. S7 in ESI). However, it is a different scenario, when the PBS^- was intercalated into LDH. Therefore, it can be expected that this transformation was related with the unique 2D intercalation structure of the LDH-based composite thin films. The electrostatic interactions resulted in the nucleotides anions approached to the positively charged LDH layer, diffused into the interlayer and resulted in the the hydrogen-bonding[30] interaction between the nucleotide and PBS anions. At the physiological conditions, ATP was tetavalent anion, ADP and AMP were trivalent and divalent anions, respectively. Therefore, the electrostatic force of ATP anions to LDHs layers was strongest among three AXP anions. ADP, the second, and AMP the least. The proposed mechanism scheme of the fluorescence response to AXP was illustrated in Fig. 8, in which multiple hydrogen bonds can be established betweeen the PBS and nucleotides. This was also the case for other nucleotides (UXP; CXP; GXP) (Fig.S6**).** It can be expected that the hydrogen bonding supramolecular interactions between PBS and nucleotides occurred within the interlayer space of LDH, which resulted in the structural change of the intercalated PBS anions and the blue shift of fluorescence**.** When compared the fluorescence of PBS/LDH and ATP@PBS/LDH, it is found that the fluorescence of ATP@PBS/LDH is blue shifted for about 40 nm (Fig. S8 in ESI), which is consist with the fluorescence response of PBS(15%)-DES/LDH to ATP. Above all what we proposed about the mechanism luminescence response of PBS-DES/LDH thin film for ATP is possible correct.

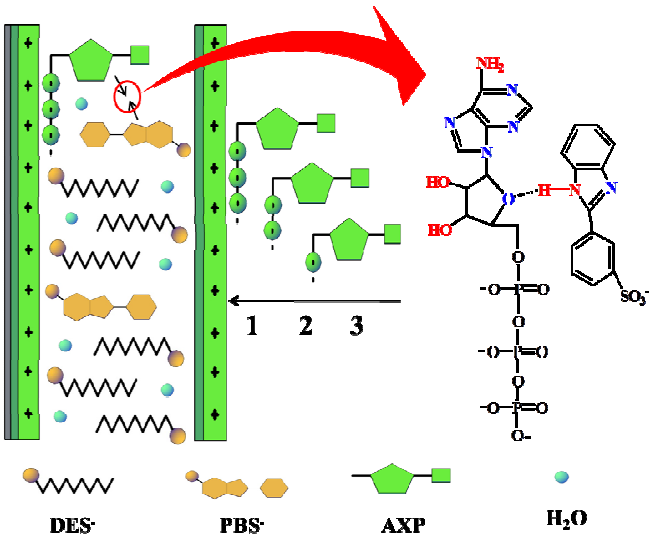

Fig. 8 The proposed mechanism scheme of the fluorescence response to AXP sollution in PBS(15%)-DES/LDH thin film, and the expected hydrogen bond modes between PBS and ATP, the hydrogen bond donor and acceptor atoms were marked in red and blue color, respectively.

Conclusions

In summary, a cheap UV light absorber, 2-phenylbenzimidazole-5-sulfonate (PBS) was immobiled into the interlayers of Zn_2Al layered double hydroxides(LDHs) by co-intercalating with 1-decane sulfonate (DES) anions. The fluorescence dependance on the molar concentrantion (*x*%) of PBS was investigated and it was found that the PBS(15%)-DES/LDH composite exhibits the optimal violet luminescence at 402 nm, compared with that of PBS solution with luminescence at 342 nm. Moreover, the PBS(15%)-DES/LDHs thin film was fabricated, and its special fluorescence response to the nucleotide presence was discovered and most remarkble for nucleotide triphosphates, due to the particular hydrogen bonding interaction between nucleotides and the intercalated PBS. This transformation was repeatably, rapid, and universal for other nucleotides (UXP, CXP and GXP) and can be used as the nucleotides fluorescence sensors. In a word, a new fluorescence sensing method and sening prototype system were developed for nucleotides detection based on the solid thin film device of

intercalated LDHs, which provides the potential applications in biological molecules detection.

Acknowledgements
This work was supported by the 973 Program (Grant No.: 2014CB932101), the National Natural Science Foundation of China, 111 Project (Grant No.: B07004), Program for Changjiang Scholars and Innovative Research Team in University (IRT 1205), and New Century Excellent Talents in University (NCET-11-0560) Electronic Supplementary Information is available online or from the author.

References

1 R. Martinez-Manez and F. Sancenon, *Chem. Rev.,* 2003, **103**, 4419.
2 Z. Xu, S. K. Kim and J. Yoon, *Chem. Soc. Rev.,* 2010, **39**, 1457.
3 P. A. Gale, *Chem. Soc. Rev.,* 2010, **39**, 3746.
4 S. K. Kim and J. L. Sessler, *Chem. Soc. Rev.,* 2010, **39**, 3784.
5 A. F. Li, J. H. Wang, F. Wang and Y. B. Jiang, *Chem. Soc. Rev.* ,2010, **39**, 3729.
6 Z. Xu, X. Chen, H. N. Kim and J. Yoon, *Chem. Soc. Rev.,* 2010, **39**, 127.
7 Z . Xu , N. J. Singh, J. Lim, J. Pan, H. N. Kim, S . Park, K . wang, S. Kim , and J. Yoon，*J. Am. Chem. Soc.,* 2009 , **131**,15528.
8 Y. Zhou, Z. Xu and J. Yoon, *Chem. Soc. Rev.,* 2011,**40**, 2222
9 A. V. Gourine, E. Llaudet, N. Dale and K. M., *Spyer, Nature,* 2005, **436**, 108.
10 B. Alberts, A. Johnson, J. Lewis, M. Raff, K. Roberts and P. Walter, in *Molecular Biology of the Cell* Garland Science, New York, 2002.
11 S. M. olz, D. C. Tharine, H. Decker and C. I. Tasca, *Brain Res.,* 2008, **113**,1231.
12 D. Lecca and S. Ceruti, *Biochem. Pharmacol.,* 2008, **75**, 1869.
13 C. Bazzicalupi, S. Biagini, A. Bencini, E. Faggi, C. Giorgi, I. Matera and B. Valtancoli, *Chem. Commun.,* 2006, 4087.
14 C. Li, M. Numata, M. Takeuchi and S. Shinkai, *Angew. Chem. Int. Ed.,* 2005, **44**, 6371.
15 M. Ogawa and K. Kuroda, *Chem. Rev.,*1995 , **95** , 399.
16 D. P. Yan, J. Lu, J. Ma, M. Wei, S. D. Li, D. G. Evans and X. Duan. *J. Phys. Chem. C*, 2011, **115**, 7939
17 G. R.. Williams and D. O'Hare, *Mater. Chem.*, 2006, **16**, 3065.
18 A. M. Fogg, A. J. Freij and G. M. Parkinson, *Chem. Mater.*, 2002, **14**, 232.
19 C. J. Wang, Y. A. Wu, R. M. Jacobs, J. H. Warner, G. R Williams and D. O'Hare, *Chem. Mater.*, 2011, **23**, 171.
20 X. Duan and D. G. Evans, *Chem. Commun.*, 2006, 485.
21 J. B. Han, J. Lu, M. Wei, Z.L. Wang and X. Duan, *Chem.Commun.,*. 2008, **41**, 5188.
22 S. Aisawa , Y. Ohnuma , K. Hirose, S. Takahashi,H. Hirahara , E. Narita , *Applied clay science*, 2005, **28**, 137.
23 H. Nakayama , A. Hatakeyama, M. Tsuhako, *Inter. J. of Pharmaceutics*, 2010, **393**, 105.
24 Y. J. Lin，Z. J. Tuo, H. Chai, D . G. Evans, D . Q. Li, *Chinese J. of Inorg. Chem.,* 2006, **22**, 1431
25 J. C. I. Liu and J. C. Bailar, *J. Am. Chem. Soc.*, 1951, **73**, 5432.
26 S. D. Li, J. Lu, J. Xu, S. Dang, D. G. Evans and X. Duan，*J. Mater. Chem.,*2010, **20**, 9718.
27 X. M. Xie, *J. Inorg. Mater.,*1999, **14**, 245
28 (a) R. Ballardini, G. Varani, M. T. Indelli, F. Scandola, *Inorg. Chem.* 1986, **25**, 3858; (b) B. D. Muegge, S. Brooks, M. M. Richter , *Anal. Chem.* 2003, **75**, 1102.
29 D. P. Yan , J. Lu, J. Ma , M. Wei, S.H. Qin , L. Chen , D. G. Evans and X. Duan , *J. Mater. Chem.*, 2010, **20**, 5016.
30 H. Wang and Wing-Hong Chan , *Org. Biomol. Chem.,* 2008, **6**, 162.

